

Supplementary Materials

1. Computational details

The molecules are connected to two slabs representative of an (111) gold surface and containing 3 layers (on the left side) and 4 layers (on the right side) of 16 (4 x 4) gold atoms to form the central scattering region. The number of gold layers has been carefully chosen to ensure the convergence of the transmission spectrum. The asymmetry (3 and 4 gold layers at different sides) is introduced for connectivity reasons. The (111) gold surface is constituted by a 3-layer cell (ABC) repeated periodically in the Z direction with a discontinuity at the scattering region. To ensure that the molecule is bonded to a top atom of the C layer on both sides, we can use the asymmetric or mirror junction options, respectively:

...ABCABC/ABC-Molecule-CABC/ABCABC...

...ABCABC/ABC-Molecule-CBA/CBACBA...,

where the slash (/) marks the frontier between the scattering region and the part of the system considered as bulk. With a mirror configuration, problems of convergence for the initial guess of the density done for a calculation on an equivalent closed and periodic bulk system: (ABC/ABC-Molecule-CBA/CBA)*n* often occur due to the creation of a double AA layer on each side by the periodic boundary conditions. This is the essential reason for the asymmetric choice. On the other hand, the asymmetry has no influence on the calculations, once enough gold layers are introduced on both sides of the molecule in the scattering region. This is needed to ensure the continuity between the gold bulk potential and gold-molecule surface potential.

The sulfur atoms are anchored on the top position on the gold surface with an Au-S distance fixed at 2.42 Å. For the meta-phenylene linker, this anchoring required the removal of two gold atoms on each surface to prevent steric hindrance with the external hydrogen atom. This does not induce any significant changes in the calculated transport properties, as verified for the para-phenylene linker with or without two gold atoms removed. We have not considered other anchoring positions since we are primarily interested here in understanding the parameters controlling the ON/OFF ratio in a model molecular junction; moreover, the actual contact geometry is often ill-defined in nanojunctions.

This central scattering region is coupled to semi-infinite electrodes on each side to compute the electronic structure and the transmission spectrum of the junctions using the Non-Equilibrium Green's Function formalism based on the DFT method, as implemented in the ATK2008.10 package. The use of Green's functions allows us to extract electronic properties of a system which is non-periodic in the transport direction while the transverse x,y directions are treated periodically [1]. The exchange-correlation is treated with the GGA.revPBE functional. GGA functionals like this one are known to underestimate molecular HOMO-LUMO gaps, because of the lack of derivative discontinuity. Incidentally, this gap reduction can account for molecular gap renormalization in the vicinity of metal surface by image effects [2]. However, this renormalization can be excessive and leads, in transmission calculations, to current overestimation by positioning the transmission peaks originating from frontier MOs too close to the Fermi level. Still, there are all grounds to believe that the identification of the transmission pathways remains correct [3], as well as the relative current values for similar molecules. Moreover, the pinning effect at the heart of our manuscript makes the initial HOMO-LUMO gap (and hence the functional) not critical to define the level alignment. The basis set is SZP for valence gold electrons, DZP for valence electrons of the molecule, a 7 x 7 x 50 k-point sampling and a mesh cut-off of 180Ry within the SIESTA scheme[1]. The core electrons are frozen and implicitly included in norm-conserving Troullier-Martins pseudopotentials [4,5]. In a last step, the I-V characteristics are obtained from the transmission probabilities $T(E,V)$, a function of the energy and of the applied bias, on the basis of Landauer's formula:

$$I(V) = \frac{2e}{h} \int T(E,V)(n_D(E, \mu_L) - n_D(E, \mu_R))dE$$

The difference between the Fermi-Dirac statistics, n_D , in the two electrodes, induced by the difference in chemical potentials triggered by the applied bias, defines a transmission window throughout the device. The current is integrated within this transmission window between the Fermi levels of the electrodes associated to the chemical potentials (Figure S1).

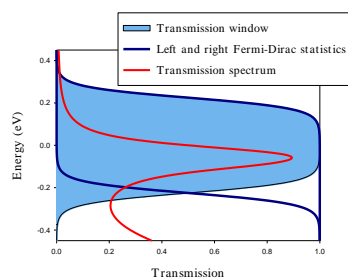


Fig. S1: Graphical illustration of the Landauer's formula. The zero of energy is set to the average Fermi level of both electrodes. The Fermi-Dirac statistics of the left and right electrodes are reported for an applied bias of 0.45V at 300K. Their difference defines the blue zone which represents the transmission window. A transmission spectrum with a peak lying near the Fermi level is also depicted. Only the part of this peak located inside the transmission window will participate to the current upon integration. Note that our quantum-chemical calculations are performed at 300 K.

2. Isolated molecules: frontier orbitals

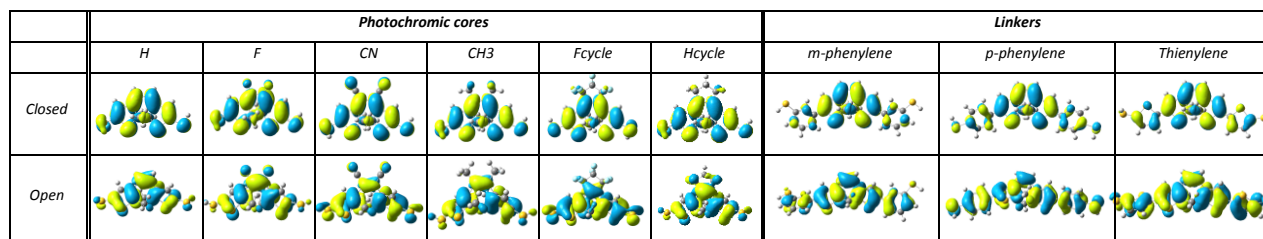


Fig. S2: Shape of the HOMO level in all derivatives in both the open and closed forms, as provided by the DFT-B3LYP calculations. The isocontour value has been set to 0.02.

For the isolated molecules, we have optimized the molecular geometry at the hybrid DFT B3LYP/6-31G** level with Gaussian 03 and analyzed the shape and energy of the frontier molecular orbitals at the same level. However, for the sake of consistency, we have also calculated the frontier MO energies at the same level of theory as that used in ATK2008.10 for the junction properties, i.e. pure DFT GGA.revPBE/DZP. We compare the energies in Fig. S3 and give HOMO topologies in Fig. S4. It is clear that GGA.revPBE/DZP calculations yield the same trends for the substituent effects, in spite of systematic underestimation of the gap typical for pure DFT functionals. Also HOMO orbital topologies are compatible after comparison with Fig. S2. Therefore, it is coherent to extend the reasoning based on B3LYP/6-31G** calculations on molecules to the junctions.

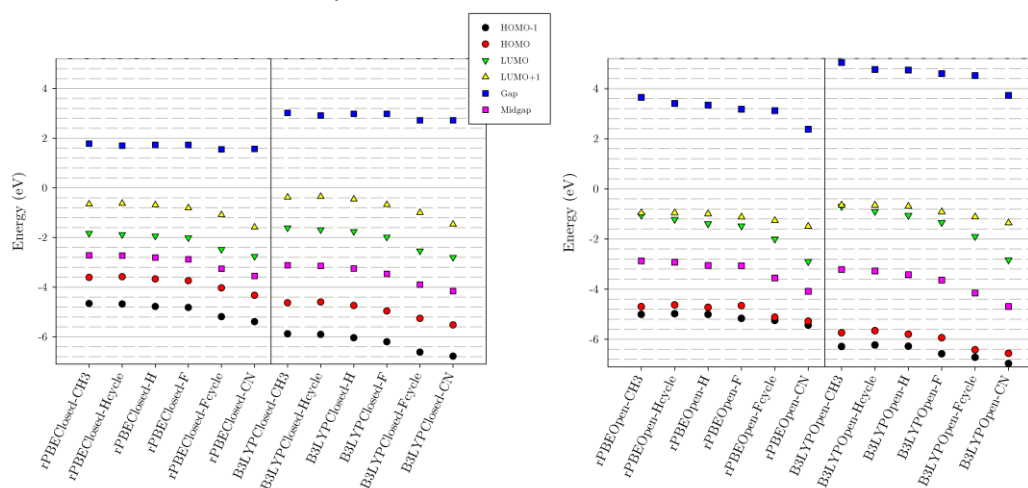


Fig. S3: Comparison between GGA.revPBE/DZP and B3LYP/6-31G** energy spectra calculations.

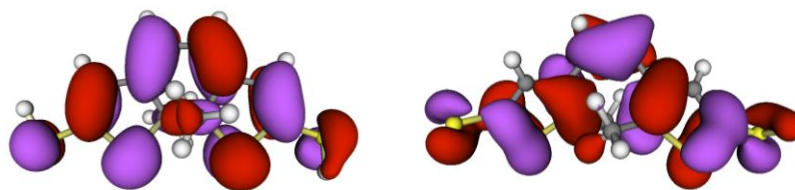


Fig. S4: HOMO frontier orbitals as calculated with ATK2008.10 at GGA.revPBE/DZP DFT level.

References:

- 1 J. Soler, E. Artacho, J. D. Gale, A. Garcia, J. Junquera, P. Ordejón and D. Sanchez-Portal, *J. Phys.:Condens. Matter*, 2002, **14**, 2745.
- 2 B. Neaton, M. S. Hybertsen and S. G. Louie, *Phys. Rev. Lett.*, 2006, **97**, 216405.
- 3 S. Y. Quek, L. Venkataraman, H. J. Choi, S. G. Louie, M. S. Hybertsen and J. B. Neaton, *Nano Lett.*, 2007, **7**, 3477
- 4 G. B. Bachelet, D. R. Hamann and M. Schlüter, *Phys. Rev. B*, 1982, **26**, 4199.
- 5 N. Troullier and J. L. Martins, *Phys. Rev. B*, 1991, **43**, 1993.